Journal of Colloid and Interface Science 542 (2019) 222–232

Contents lists available at ScienceDirect

Journal of Colloid and Interface Science

journal homepage: www.elsevier.com/locate/jcis

Regular Article

Interfacial properties, film dynamics and bulk rheology: A multi-scale approach to dairy protein foams

Alexia Audebert [a], Arnaud Saint-Jalmes [b], Sylvie Beaufils [b], Valérie Lechevalier [a], Cécile Le Floch-Fouéré [a], Simon Cox [c], Nadine Leconte [a], Stéphane Pezennec [a,*]

[a] STLO, UMR1253, INRA, Agrocampus Ouest, F-35000 Rennes, France
[b] Univ Rennes, CNRS, IPR (Institut de Physique de Rennes) - UMR 6251, F-35000 Rennes, France
[c] Department of Mathematics, Aberystwyth University, Ceredigion SY23 3BZ, Wales, UK

GRAPHICAL ABSTRACT

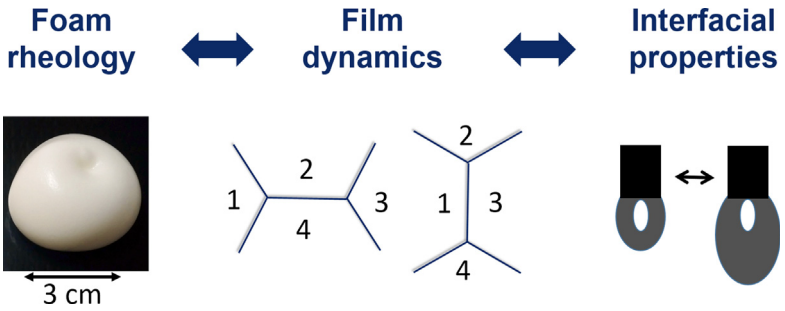

ARTICLE INFO

Article history:
Received 17 October 2018
Revised 31 January 2019
Accepted 1 February 2019
Available online 2 February 2019

Keywords:
Foam rheology
Interfacial rheology
Topological rearrangement
Disproportionation
Whey protein
Powder dry-heating

ABSTRACT

Hypothesis: The effective contribution of interfacial properties to the rheology of foams is a source of many open questions. Film dynamics during topological T1 changes in foams, essentially studied for low molecular weight surfactants, and scarcely for proteins, could connect interfacial properties to protein foam rheology.
Experiments: We modified whey protein isolate (WPI), and its purified major protein β-lactoglobulin (β-lg) by powder pre-conditioning and dry-heating in order to obtain a broad variety of interfacial properties. We measured interfacial properties, film relaxation duration after a T1 event and bulk foam rheology.
Findings: We found that, for β-lg, considered as a model protein, the higher the interfacial elastic modulus, the longer the duration of topological T1 changes and the greater the foam storage and loss moduli and the yield stress. However, in the case of the more complex WPI, these correlations were less clear. We propose that the presence in WPI of other proteins, lactose and minerals modify the impact of pre-conditioning and dry-heating on proteins and thereby, their behaviour at the interface and inside the liquid film.

1. Introduction

Liquid foams are concentrated dispersions of gas bubbles into a liquid. The mechanical behaviour of foams combined with their low density and large interfacial area lead to a wide variety of industrial applications: flotation, oil production, firefighting, food and cosmetic products [1,2]. However, the use of liquid foams in industry is restricted due to destabilisation processes such as drainage, disproportionation and coalescence [1–4]. Foam drainage is the flow of liquid under the influence of gravity through the network of films and Plateau borders. Coalescence is the fusion of two bubbles after the rupture of a liquid film or lamella separating them. Disproportionation is the result of the diffusion of gas

* Corresponding author.
E-mail address: stephane.pezennec@inra.fr (S. Pezennec).

https://doi.org/10.1016/j.jcis.2019.02.006
0021-9797/

between bubbles, driven by gradients of Laplace pressure. Drainage leads to a drier foam (a decrease of the foam liquid fraction ϕ) whereas coalescence and disproportionation both lead to larger average bubble size R (although with a different size distribution) [2,3].

From a rheological point of view, a foam behaves as a solid or a liquid depending on the applied strain (Fig. 1). When a small strain is applied to a foam sample, the bubbles are deformed and thus their interfacial area and interfacial energy increase, giving rise to an elastic stress. If the applied strain is increased beyond the yield strain (respectively, if the stress is increased above a yield stress), bubbles start to rearrange and the foam flows. The yield strain corresponds to the onset of plastic events, i.e. irreversible bubble rearrangements, called T1s, represented by the transition from configuration (a) to configuration (d) in Fig. 1. The macroscopic yielding and flow of a foam are analysed in terms of succession of T1 events, at the scale of the bubbles [5–7]. Note that even without an applied stress, T1 are also triggered by disproportionation [5,6]. T1 events are also related to foam coalescence, since film rupture may occur during the bubble rearrangement [8–10]. Despite the fact that T1s are increasingly considered as crucial in foam rheology and stability, the links between the dynamics of the T1 (duration of the rearrangement) and the foam dynamical properties are not yet clarified.

The foaming of a solution is helped by adding surfactants, which first decrease the gas-liquid interfacial tension. In addition, surfactants promote the foam stability, by providing rheological properties to the gas-liquid interfaces, and by inducing repulsive forces between bubbles.

Still, the effective contribution of interfacial properties to the stability and rheology of foams is a source of many open questions. Indeed, foam dynamics resulting from the occurrence of simultaneous and interdependent instability mechanisms make correlations between length scales far from trivial [11–13].

Proteins are amphiphilic macromolecules, which adsorb to hydrophobic interfaces and are able to stabilise foams and emulsions. But, in contrast with LMW surfactants, proteins may undergo conformational changes and self-assemble at the interface, leading to the formation of a dense, visco-elastic layer. This feature discriminates proteins from LMW surfactants, though making the relationship between interfacial concentration and interfacial tension more complex [14]. Secondly, protein adsorption at the interface can be considered almost irreversible, due to the large number of adsorbed protein segments at the interface. Interfacial protein self-assembly and quasi-irreversibility of the adsorption may result in low-frequency shear and dilatational viscoelasticity, while these features are not found for LMW surfactants. Consequently, the specific interfacial behaviour of proteins can be useful to implement our understanding of the link between interfacial rheology and foam properties.

Even if proteins are not easy to characterise because they often have non-equilibrium interfacial properties, some investigations of the link between interfacial and foam properties have been performed. Interfacial dilatational parameters have been used to explain foamability and stability at short times [14,15]. Stability against disproportionation has also been correlated with the higher interfacial dilatational elasticity E' of proteins [15]. Concerning foam rheology, it has been shown for β-lactoglobulin (β-lg) that a higher dilatational and shear interfacial elasticity can increase the yield stress and storage modulus of a foam [16].

Lastly, another specific feature of proteins is that they have a three-dimensional structure responsive to environmental physicochemical conditions (pH, ionic strength, heating...) [17]. Globular proteins, for instance whey proteins, have different gas-liquid interfacial properties depending on the protein structure [18–21]. For this reason, many processing technologies, especially heat treatments, have been applied to whey proteins in order to change their structure, and consequently their interfacial properties [22].

In this work, we have investigated different protein systems and used different processes to modify their properties. We used whey protein isolate (WPI) and its purified major protein β-lactoglobulin (β-lg), and compared them to another milk protein fraction, sodium caseinate, which is known to exhibit relatively low interfacial visco-elasticity. Dry-heating WPI and β-lg powders in various conditions was used to obtain an even broader range of interfacial properties [23,24]. Indeed, our previous work has shown that powder dry-heating, under controlled physicochemical conditions, does affect foam stability, which suggests that it changes the interfacial properties [25].

In parallel, we have adopted a multi-scale approach. The first level was the study of gas-liquid interfaces, combining static and dynamic measurements, namely surface tension and dilatational viscoelasticity. The second level was the characterisation of the dynamics of films between bubbles, through the duration of T1 rearrangement events, using a five-film setup. Finally, we studied the rheology of foams through oscillatory measurements to determine the yielding of the foams, and their aging.

Our goal is to correlate observations at those different scales, in order to shed light on how protein formulation and processing affect interfacial and film properties, and to understand how the latter impact the properties of foams. We also would like to bring to the attention of physicists that a wide range of interfacial rheological behaviours or foam properties may be explored by using proteins. Conversely, we also would like to raise awareness among food scientists of how some tools of foam physics can help to understand the behaviour of protein foams.

2. Materials and methods

2.1. Materials

We studied a mixture of proteins called whey protein isolate (WPI), mainly composed of β-lactoglobulin (β-lg) and α-lactalbumin (α-la). We also studied purified β-lg, as a model

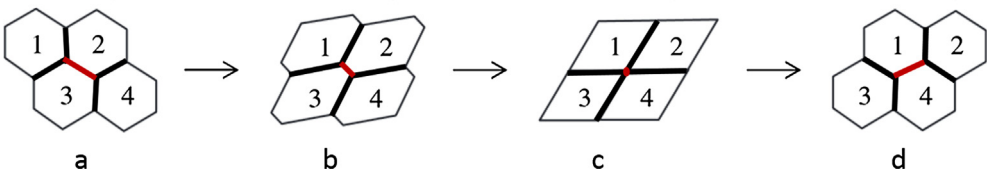

Fig. 1. Topological T1 rearrangement. An increasing shear strain is applied to a 2D foam structure, where four bubbles are separated by five films (thick segments). From (a) to (b), bubbles are deformed, interfaces store elastic energy and the central film (in red) is shrunk. Configuration (c) is an unstable intermediate configuration in which the four lateral films meet at a point. From (c) to (d), spontaneously, a new central film (in red) is created and then stretched until a static equilibrium configuration is reached, in which any three films meet at 120° due to the area minimisation according to Plateau's law. The topological T1 rearrangement consists in the transition between configurations (a) and (d), leading to a bubble neighbour switching. Adapted from Höhler and Cohen-Addad [5]. (For interpretation of the references to colour in this figure legend, the reader is referred to the web version of this article.)

protein. Sodium caseinate (NaCas) from Armor Protéines (Saint-Brice-en-Coglès, France) and sodium dodecyl-sulfate (SDS) from Sigma-Aldrich (Saint-Quentin, France) were also used for comparisons, as they are expected to have low or no interfacial viscoelasticity.

β-lg was purified from bovine milk by using pilot-scale membrane separation technology, in which the temperature did not exceed 56 °C in order to preserve its native structure [26–28]. Fresh unheated milk was skimmed and microfiltrated (1.4 μm), and then caseins were separated from the whey by microfiltration (0.1 μm). The whey protein solution was concentrated by ultrafiltration (5 kDa), diafiltrated with deionised water, and then was subsequently frozen until further purification. Then, the thawed whey protein solution was acidified to pH 3.8 using citric acid and heated (56 °C) to precipitate α-lactalbumin. After microfiltration (0.1 μm), the microfiltrate containing β-lg was concentrated by ultrafiltration (10 kDa), diafiltrated with deionised water and freeze-dried. The β-lg concentration was determined by UV absorption using a specific extinction coefficient of 0.96 $mL{\cdot}g^{-1}{\cdot}cm^{-1}$ at 280 nm [29]. Freeze-dried β-lg contain 77.3% ± 1.7% of β-lg.

WPI powder was obtained by spray-drying a whey protein concentrate isolated from milk microfiltrate by ultrafiltration and diafiltration as described by Chevallier et al. [30]. The nitrogen content (TN), non-protein nitrogen (NPN) content and non-casein nitrogen (NCN) content of the powder were determined by the Kjeldahl method [31]. The protein content P was calculated using:

$$P = (TN - NPN) \times 6.38 \quad (1)$$

The amount CN of casein or insoluble proteins at pH 4.6 was measured using:

$$CN = (TN - NPN - NCN) \times 6.38 \quad (2)$$

Free lactose in the WPI powder was measured by ion-exchange high performance liquid chromatography (HPLC, Dionex, Germering, Germany) using an Aminex A-6 column (Biorad, St Louis Mo., USA) and a differential refractometer (model RI 2031 plus, Jasco). The oven was kept at 60 °C and the elution flow was 0.4 $mL{\cdot}min^{-1}$ using 5 mM H_2SO_4.

We determined that WPI powder contained 95.0 ± 0.2% (w/w) of protein (using Eq. (1)), of which 9.40 ± 0.04% (w/w) consisted of caseins or insoluble proteins at pH 4.6 (calculated using Eq. (2)). WPI contained also 2.04 ± 0.02% (w/w) free lactose.

2.2. Sample preparation

Spray-dried WPI and freeze-dried β-lg were each dissolved in deionised water. In order to reduce the amount of caseins and insoluble proteins (particularly for the WPI samples), they were adjusted to pH 4.6 by adding 12 N HCl and centrifuged for 30 min at 9000×g (Fig. 2). In that way, the amount of casein and insoluble proteins in the supernatant collected from WPI was reduced from 9.4% to 5.89%. The solutions were then adjusted to pH 3.5 or pH 6.5 using 12 N HCl or 12 N NaOH and lyophilised. Then, the water activity a_w of lyophilised powders was adjusted to 0.23, corresponding to a common value for commercial dairy powders, by storing them for 2 weeks at room temperature in an airtight vessel also containing a saturated $MgCl_2$ solution. The water activity of powders before and after dry-heating was checked using an a_w-meter (Novasina, Axair Ltd, Switzerland). Powders with adjusted pH and a_w were dry-heated at 70 °C for 0 or 125 h in hermetically sealed bags. The powders were then solubilised in deionised water at a protein concentration of 50 g/L and adjusted to pH 7.0. It should be noted that all the experiments were performed at the same protein concentration 50 g/L, enabling a direct comparison between different samples, and at room temperature.

In the following, we have differentiated untreated samples from processed samples (Fig. 2). The processed samples underwent the pre-conditioning step, either with or without subsequent dry-heating.

2.3. Dynamic drop tensiometry and interfacial dilatational rheometry

A pendant drop tensiometer (Tracker, from Teclis-Scientific, France) was used to determine the dynamic interfacial tension at the solution-air interface using a 50 g/L protein solution. After

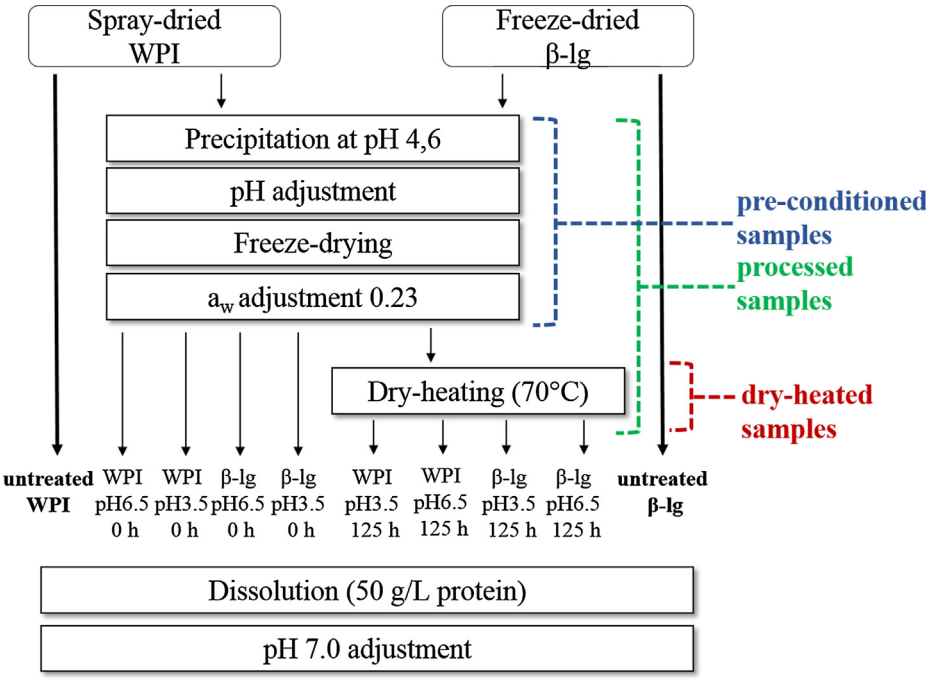

Fig. 2. Protein sample preparation.

formation of a fresh liquid drop hanging from the tip of the needle, the time evolution of the interfacial tension was followed for 1600 s by drop shape analysis, with the drop maintained at a constant 7 μl volume.

The same setup was used for interfacial dilatational rheometry. In order to measure the complex interfacial dilatational modulus (E), sinusoidal drop oscillations (with amplitude ±0.75 μl, pulsation $\omega = 1.26$ rad/s) were applied and the interfacial tension response was recorded. Since the surface area of the drop oscillates periodically, the dilatational modulus E exhibits two contributions: the storage modulus, E', and the loss modulus, E'' which accounts for the energy lost through relaxation processes. We report the dilatational moduli E' and E'' at two different times (250 s and 1600 s) in Table A (supplementary data), obtained by two methods. Firstly, the time evolution of the dilatational moduli were obtained by applying to a freshly formed drop continuous oscillations as a function of time until an aging time of 1600 s. Differences between samples were higher at 250 s than at 1600 s. Thus, we only report the values $E'_{250\ s}$ and $E''_{250\ s}$ of dilatational moduli at 250 s. Secondly, to avoid continuous oscillations for long times and possible perturbation of the protein layer, we imposed only few periods of oscillation after a 1600 s aging to obtain $E'_{1600\ s}$ and $E''_{1600\ s}$.

2.4. T1 Dynamics

The T1 process corresponds to the transition between two equilibrium film structures illustrated as configurations (a) and (d) in Fig. 1. We studied the relaxation of the films following the change of topology by measuring the length of the new central film as a function of time until static equilibrium is reached (Fig. 1, configurations (c) to (d)).

Our "five-film" setup to explore the dynamics following a T1 is composed of two perspex plates separated by four fixed pins. Two further, moveable, pins are attached to a rod that can move back and forth across the device. By immersing the device into the protein solution, five films were created, attached to two of the fixed pins and the two mobile pins, as shown in Fig. 3. An initial configuration as in Fig. 3, left, was obtained; this sometimes required gentle blowing on the films to cause them to rearrange. The rod was then moved towards the fixed pins, causing the central film to shrink until an unstable configuration was reached and a T1 occurred. The relaxation of the films after the T1 rearrangement (Fig. 3, right) was recorded at 25 frames per second by a video camera fixed vertically above the device (see the movies provided as Supplementary data). To increase the image contrast, the device was placed on a black background and lit from above. Image processing with ImageJ allowed us to determine the length L of the newly-created film as a function of time. We present results for this length normalised by its final length L_∞ [32]. We characterised the relaxation duration using the time t_{90} necessary for the film to reach 90% of its final length L_∞ [33].

The liquid contents of the menisci (known as Plateau borders) and the film were not controlled, but the central film thickness was monitored by image analysis.

2.5. Foam formation and rheometry

The two-syringe technique was used to obtain liquid foams [34,35]. The liquid fraction ϕ, defined as the ratio V_{liquid}/V_{foam} of the liquid volume to the total foam volume, was fixed at 0.16. ϕ is controlled by the ratio of the initial amount of the liquid and the total volume of the two syringes. Foams were all produced after twenty plunges of the syringes.

Foam rheology measurements were performed on the freshly produced foams using a rheometer (MCR301, Anton Paar) with a 75 mm cone-plate geometry. The viscoelastic shear moduli G' and G'' and the yield strain γ_c were measured during an oscillatory amplitude sweep from 1 to 50% strain with a frequency of 1 Hz. We define G'_0 and G''_0 as the moduli at a strain $\gamma = 1\%$. The yield strain γ_c was defined as the strain at which the viscous properties start to dominate over the elastic ones, i.e. the crossover of G' and G''. The yield stress τ_c was then calculated from:

$$\tau_c = \gamma_c \cdot G'_0 \quad (3)$$

where γ_c the yield strain and G'_0 the foam storage modulus in the linear viscoelastic regime of the foam [36].

The shear modulus G' was also recorded as function of the foam aging time at constant frequency 1 Hz and strain $\gamma = 1\%$.

2.6. Bubble size characterisation

Bubble size was measured by the bubble raft method. Freshly-produced foams were deposited inside a Petri dish containing the same protein solution used to make the foam (Fig. A in supplementary data). A mean bubble radius was manually calculated over four images of the same foam.

2.7. Statistical analysis

Adjustments for multiple comparisons using Tukey's tests were performed to test the significance of mean differences between protein samples (p-values < 0.05). Correlations between different

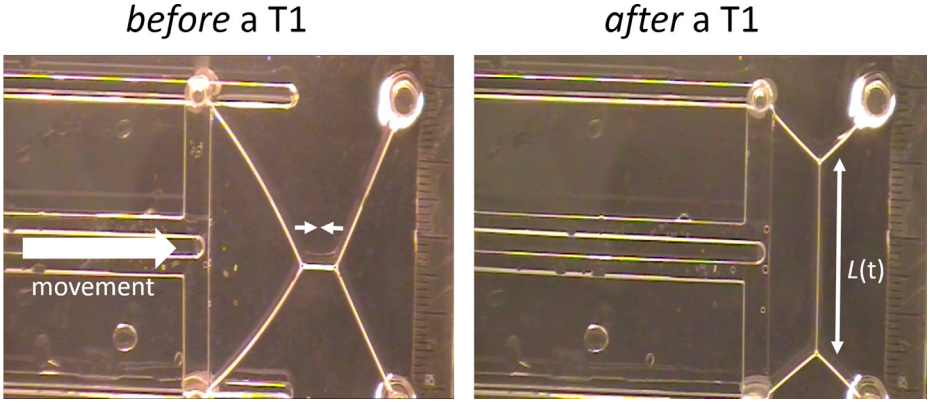

Fig. 3. Five-film setup for T1. The four-bubble foam illustrated in Fig. 1 is simplified to the five films indicated by thicker segments in Fig. 1, confined between two perspex plates and viewed from above. The five films are stretched between two fixed pins and two mobile pins. The T1 event is triggered by moving the two mobile pins from left to right. The length *L(t)* of the new central film created after the T1 event is measured as a function of time. These pictures are extracted from a movie showing the whole process, provided as supplementary data.

parameters were determined using Spearman's rank correlation test (coefficient r_s). Data were analysed using the R software package [37].

3. Results

The results section introduces essentially raw experimental data, detailed scale by scale: (i) single interface, (ii) films dynamics, and (iii) tridimensional foams. The possible correlations between them are presented in the Discussion section.

3.1. Characterisation of interfacial properties

The real and imaginary parts of the viscoelastic interfacial dilatational modulus (E', E") were measured as a function of time for different samples (Fig. 4). NaCas had a low viscoelastic modulus in comparison with untreated β-lg and WPI. At early times (t < 100 s), NaCas and WPI behaved quite similarly but then diverged significantly as time increased. The modulus for untreated β-lg and WPI steadily rised with time, probably because of evolving inter-protein interactions. In addition, untreated β-lg showed higher moduli than untreated WPI.

Further, Fig. 5 shows the time evolution of interfacial moduli for β-lg (a, b) and WPI (c, d) samples before and after processing. Interestingly, the dilatational moduli at early times differentiates the samples significantly more clearly than at longer times. For this reason, interfacial properties have been characterised at both early and longer times (250 s and 1600 s). We note that in most cases the value of E" did not exhibit a well-pronounced plateau, but instead continuously declined, as observed by Ulaganathan et al. [38]. In other words, $E"_{250\ s} > E"_{1600\ s}$ for most of the samples. In addition, the time evolution of the moduli for β-lg was faster than for WPI samples, whatever the treatment (see also Table A, Supplementary data). Interestingly, untreated WPI and β-lg samples (represented with black lines in Fig. 5) differed from the processed samples, either dry-heated or not. Hence, the powder pre-conditioning step prior to dry-heating significantly changed the interfacial properties of the reconstituted solutions described in Fig. 2. Fig. 5 also illustrates that pre-conditioning and dry-heating effects depended on the sample composition (β-lg or WPI). As an example, the maximum values for $E'_{250\ s}$ were obtained after pre-conditioning at pH 6.5 for β-lg (≈ 65 mN/m) and pH 3.5 for WPI (≈ 60 mN/m) (Fig. 5a and c). In addition, powder dry-heating increased the imaginary part E" for β-lg and decreased it for WPI (Fig. 5b and d). However, dry-heating of both WPI and β-lg powders significantly decreased E' whatever the pH (Fig. 5a and c).

Protein processing thus clearly impacted the interfacial rheology. In contrast, the impact of protein processing on interfacial tension was less marked (see Fig. B, Supplementary data). Table A in the supplementary data summarises all the interfacial properties by their values and standard deviations at 250 s and 1600 s.

It should be noted that the dilatational moduli were null for SDS in this frequency range (data not shown), which points at the interest of proteins as compared to LMW surfactants. For comparison, SDS gave interfacial tensions close to 36 mN/m.

3.2. Dynamics of T1 events

Fig. 6 shows typical normalised film length as a function of time during the relaxation after a T1 event for some of the samples, in order to compare (i) proteins and SDS, and (ii) whey proteins and caseinate. The relaxation corresponds to the creation and stretching of a new film until a static equilibrium is reached. As a first output, note that the relaxation was drastically faster for SDS (≈ 0.2 s) than for the protein samples (1.23 s–4.56 s). As well, the relaxation was slower with NaCas than with untreated β-lg and WPI samples.

Fig. 7 shows that the effect of pre-conditioning and dry-heating depended on the sample composition. First, processed β-lg samples had a significantly longer relaxation than processed WPI samples. Second, whereas dry-heating at pH 3.5 significantly increased the relaxation time for β-lg, it decreased it for WPI. Finally, it is worth noting that the pre-conditioning at pH 3.5 for WPI and pH 6.5 for β-lg gave rise to longer relaxation times than for untreated samples.

3.3. Foam rheology and aging

Fig. 8 shows the foam storage and loss moduli (G' and G", respectively) as a function of strain for different samples. Each foam behaved as a viscoelastic material at the lowest measured strain ($\gamma = 1\%$), G'_0 being slightly higher than $G"_0$. However, the low limit of the strain range was not low enough to clearly evidence the linear regime, where G' is independent of γ. From these plots, a yield strain γ_c can be extracted, defined as the strain at which G" first exceeds G'. The values of both G'_0 and the yield strain follow the ranking: untreated WPI > untreated β-lg > NaCas.

Upon aging, a liquid foam undergoes drainage and disproportionation. For our foams having a mean bubble diameter smaller than 60 μm and considering the small thickness of the foam samples inside the rheometer, the drainage can be considered negligible [2], and one can essentially expect disproportionation, which results in an increase of the mean bubble radius with time.

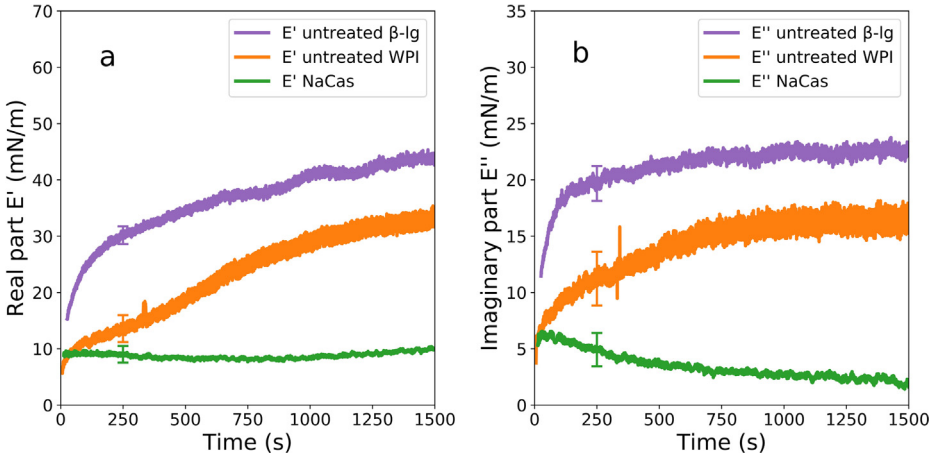

Fig. 4. Time evolution of the interfacial dilatational complex modulus for different samples: (a) real part E'; (b) imaginary part E". For each sample, the average of triplicate measurements is plotted. The error bars at 250 s show the standard deviations.

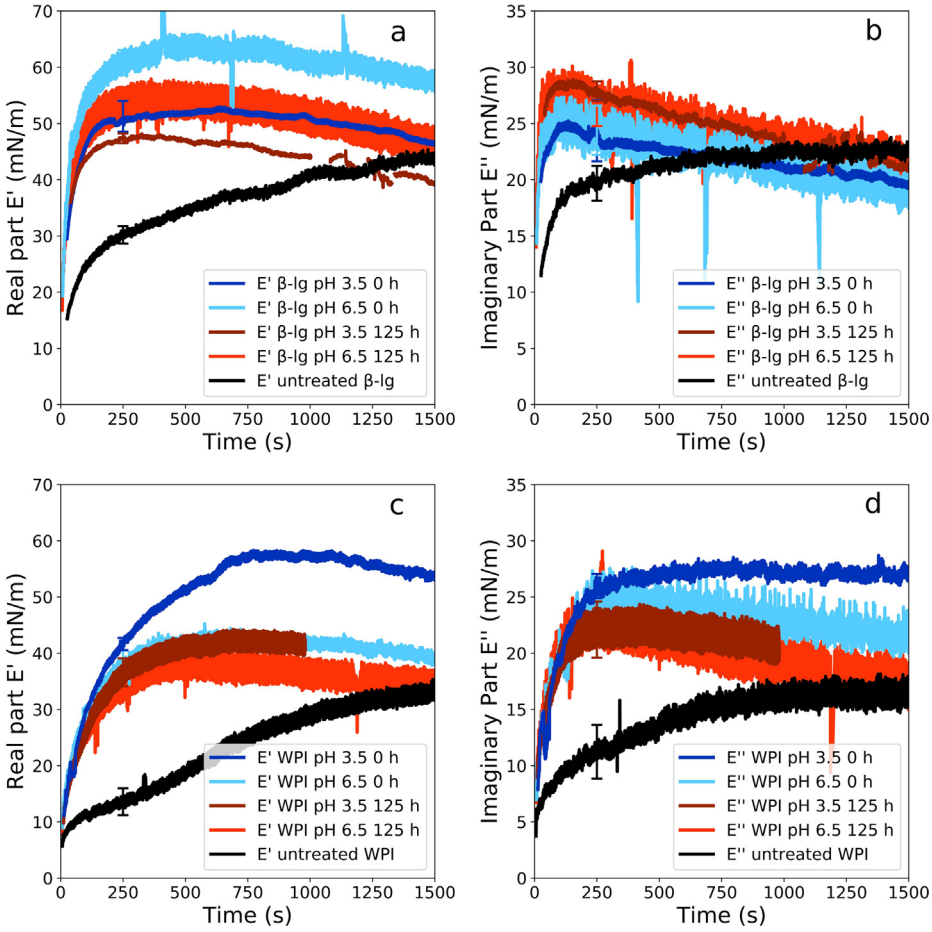

Fig. 5. Time evolution of the interfacial dilatational complex moduli (real part E', imaginary part E'') for β-lg samples (a, b) and WPI samples (c, d). Black: untreated samples; blue: pre-conditioned samples; red: dry-heated samples. Dark blue and red curves correspond to pH 3.5, whereas light blue and red curves correspond to pH 6.5. For each sample, the average of triplicate measurements is plotted. The error bars at 250 s show the standard deviations.

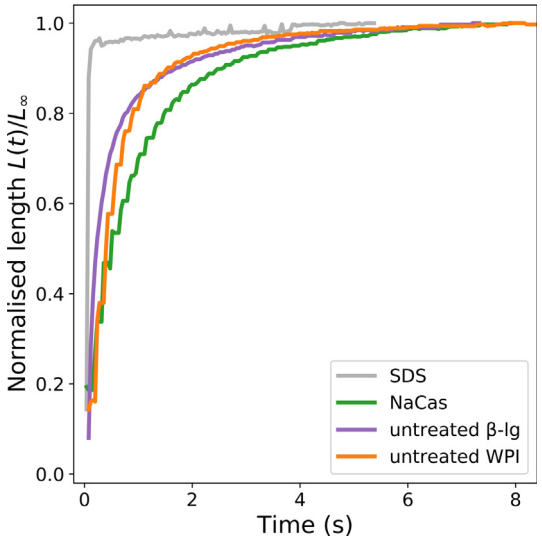

Fig. 6. Time evolution of normalised film length during the relaxation after a T1 event for different proteins and sodium dodecyl-sulfate (SDS). The film length L(t) is normalised by its final length L_∞.

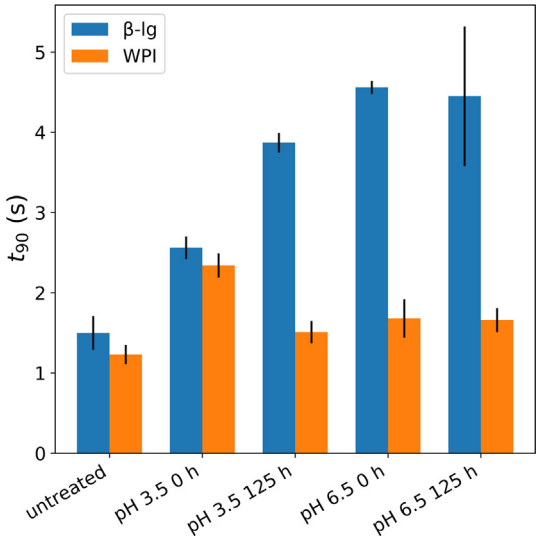

Fig. 7. Relaxation time t_{90} after a T1 for the different protein samples. t_{90} is defined as the time for the film to reach 90% of its final length. Measurements were triplicates. Error bars are standard deviations.

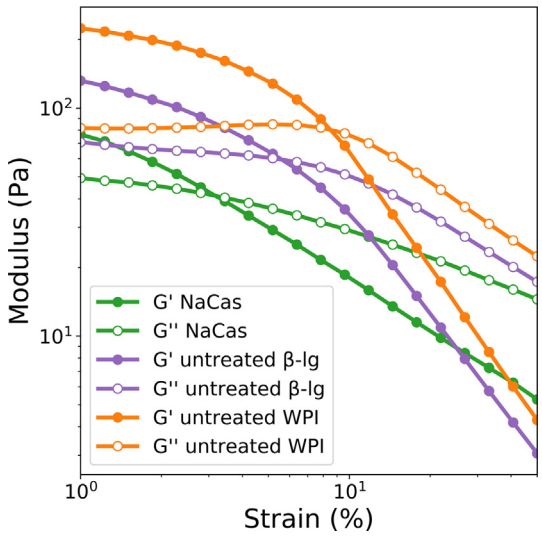

Fig. 8. Typical viscoelastic moduli for protein foams under strain-sweep oscillations at a 1 Hz frequency. Storage modulus G': closed symbols. Loss modulus G'': open symbols. Measurements were at least duplicated (see Table 1 for yield stress calculations and standard deviation).

It has been reported that the foam storage modulus G' depends on the liquid fraction and the bubble size, following:

$$G' = \frac{\sigma}{R} g(\phi) \quad (4)$$

where σ is the interfacial tension, R is the bubble radius, and $g(\phi)$ is a decreasing function of the liquid fraction [36,39,40]. Thus, without drainage, G' scales with 1/R.

Moreover, in the limit of dry foams, the bubble radius R scales with time as : $R \sim t^{1/2}$ [3,5,41–43]. Consistently, as shown in Fig. 9, $(G'_0/G'(t))^2$ increased linearly with time (after a transient initial phase), showing that disproportionation was the main cause of foam aging in those experiments.

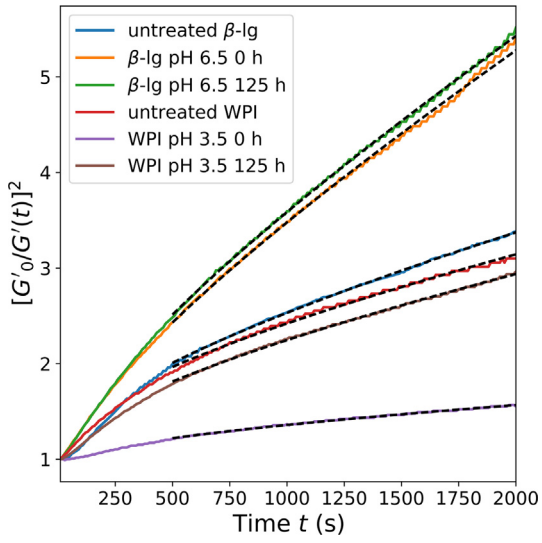

Fig. 9. Squared reciprocal of the elastic modulus G'(t) normalised by G'_0 as a function of time for different protein foams. G'_0 is the modulus value at the first measurement. Dashed black lines between 500 and 2000 s represent fitted linear functions of the square root of time. The corresponding coefficients can be considered as measurements of the disproportionation rate. Measurements were at least duplicates and typical plots are shown. Standard deviations for disproportionation rates are given in Table 1.

We therefore attribute the differences in the time-dependence of G' to differences in disproportionation rate between samples. As an illustration, pre-conditioning (samples labelled '0h' in Fig. 9) appeared to increase the disproportionation rate as compared to untreated samples for β-lg, whereas it appeared to reduce it for WPI.

To gain insight into the impact of processes on the foam bulk rheology and to compare samples quantitatively, we chose to extract the yield stress (using Eq. (3)) and the disproportionation rate from the data plotted in Fig. 8 and 9 (Table 1). The disproportionation coefficient α was obtained by fitting a linear function of the square root of time to the $G'_0/G'(t)$ data. The yield stress calculation involved intermediates quantities, which are given in Table B, in Supplementary data.

WPI samples exhibited significantly higher values of yield stress than β-lg samples, whatever the processing conditions. The yield stress was significantly higher for pre-conditioned samples than for untreated samples, whatever the sample composition (Table 1). The dry-heating and pre-conditioning effects on the yield stress depended on the protein composition (WPI or β-lg). Note also that the WPI samples had lower disproportionation coefficients than β-lg samples, whatever the processing conditions. However, whatever the sample, i.e. for β-lg as well as WPI, dry-heating increased the disproportionation coefficient.

4. Discussion

We have shown that the sample processing modified their behaviours at each scale differently depending on the sample composition (β-lg or WPI). The discussion section is composed of two parts: (i) a detailed analysis of the effects of processing and composition, including comparisons with literature data, and (ii) a study of correlations between the different scales.

The following questions will be addressed: are there some clear links between interfacial visco-elasticity, T1 duration and macroscopic foam rheology? Do they match with the literature or protein specificities? Do model experiments on T1 duration provide the same or complementary information as the interfacial characterization?

4.1. Sample composition and protein processing impact interfacial properties, film dynamics and bulk foam rheology

4.1.1. Pre-conditioning of samples accounts for the main source of differences

Whatever the sample composition, i.e. a mixture (WPI) or purified protein (β-lg), untreated samples behaved distinctly from the processed samples, either through dry-heating or pre-conditioning. Untreated samples had lower surface visco-elasticity, faster relaxation after a T1, and lower yield stress. Surprisingly, dry-heated and preconditioned samples showed similar behaviours, suggesting that pre-conditioning of the samples, though it is not expected to induce major changes in protein structure or physicochemical properties, was the main cause of the changes in sample properties. This is consistent with previous results. For instance, it has been shown that adjusting the pH prior to dehydration, followed by a_w pre-conditioning for two weeks at room temperature, significantly affected foaming properties [25].

We also think that untreated samples contain partially-altered or aggregated proteins, due to former powder storage, which impact interfacial and foam properties. Indeed, it has been shown that the storage of WPI powders significantly affects the process of protein aggregation [44]. Thus, in the present work, we used a precipitation step at pH 4.6, aiming to remove residual caseins, denatured proteins and aggregates formed upon prior processing.

Table 1
Foam bulk yield stress and disproportionation coefficient. The yield stress was calculated using the measured visco-elastic moduli, as described in Materials and methods (see Eq. (3)). The disproportionation coefficient has been evaluated by fitting a linear function of the square root of time to the evolution of the bulk foam elastic modulus G'. Measurements were at least duplicates.

Samples	Yield stress (Pa)			Disproportionation α (10^{-3}·$s^{-1/2}$)		
untreated β-lg	6.99	*±0.61*	*a*	18.20	*± 0.77*	*bc*
β-lg pH 3.5 0 h	18.66	*±1.17*	*bc*	24.27	*±1.99*	*cd*
β-lg pH 3.5 125 h	16.41	*±0.62*	*b*	29.16	*±1.72*	*d*
β-lg pH 6.5 0 h	18.96	*±1.97*	*bc*	29.88	*±3.54*	*d*
β-lg pH 6.5 125 h	22.40	*±0.29*	*cd*	38.06	*±4.23*	*e*
untreated WPI	19.36	*±2.05*	*bc*	16.18	*±0.56*	*bc*
WPI pH 3.5 0 h	26.78	*±1.10*	*d*	5.80	*±1.09*	*a*
WPI pH 3.5 125 h	39.95	*±0.53*	*e*	14.75	*±1.54*	*b*
WPI pH 6.5 0 h	37.82	*±2.47*	*e*	11.63	*±1.56*	*ab*
WPI pH 6.5 125 h	38.60	*±1.03*	*e*	15.34	*±2.07*	*b*

We think that this step contributed prominently to the impact of pre-conditioning (see Fig. 2). In addition, the processed samples have also been freeze-dried, which is known to affect the structural properties of proteins [45] and may contribute to changes in interfacial and foam properties.

4.1.2. Different behaviours depending on sample composition, independently of the process

Our results show that whatever the processing conditions, β-lg and WPI samples exhibited different properties at all scales: if one separately compares the untreated samples, the preconditioned samples, and the dry-heated ones, there were always strong differences between β-lg and WPI.

First, we have shown that β-lg samples had higher dilatational moduli than WPI samples, as also observed by Davis et al. [46]. In addition, we also observed that β-lg exhibited slower film relaxation, lower foam yield stress and faster disproportionation than WPI samples. Thus, interfacial and foam properties of WPI cannot be explained by the properties of its major protein β-lg.

Differences in interfacial properties between β-lg and WPI may be due to the rapid adsorption at the interface of the residual caseins present in WPI, which are known to yield low interfacial dilatational moduli [15]. It has been proposed that globular proteins such as BSA, and β-lg in the present work, may be viewed as hard spheres, resisting compression and giving a high interfacial elastic modulus, whereas caseins are comparable to soft spheres, yielding a low modulus [19]. The presence of α-la, another whey protein in WPI, may also weaken the protein layer at the interface as compared to purified β-lg. Indeed, it has been showed that α-la gives rise to lower values of E' than β-lg [46]. Moreover, the β-lg network at the interface can promote interfacial elasticity because of β-lg polymerisation through sulfhydryl-disulphide exchange [47]. Thus, the β-lg content in protein samples seems to be an important parameter of the interfacial dilatational rheology.

There is little literature on the rheology of foams made from dairy proteins. In agreement with Schmitt et al. [48], we found that WPI foams had a higher storage modulus G' than NaCas foams. Those authors suggested that a network can be formed across the lamellae, in which protein concentration is likely to be high, and that this causes high G'. We also found higher values of G' for WPI than for β-lg. A stronger protein network across the lamellae for WPI foams could also explain those higher G' values. α-la, present in WPI, is believed to increase the yield stress and the value of G' by contributing to a more cohesive network inside the protein layers and between them. On the other hand, it has been proposed that α-la could reduce the yield stress of foams made from WPI [46], but we did not observed this.

Some investigations on WPI disproportionation followed by bubble size as function of time report exponent values between of 1/3 and 1/2 [49], partly in agreement with our results. We are not aware of any previous disproportionation measurements comparing β-lg and WPI samples treated under the same experimental conditions. There were no significant differences between β-lg, WPI and NaCas as regards the disproportionation rates of single spherical air bubbles [50]. However, foams have closely packed bubbles, and disproportionation also depends on the bubble size, shape and number of faces [51]. Liquid film thickness could explain the faster disproportionation for β-lg samples as compared to WPI [52]. In addition, β-lg foams apparently had smaller bubbles and a lower bubble size dispersion as compared to WPI foams.

The presence of lactose and α-la in WPI may also increase the thickness of the liquid lamella due to higher steric repulsion between aggregates and glycated proteins [53,54].

Finally, WPI samples show lower disproportionation rate and higher yield stress than β-lg samples, probably due to the contribution of other components such as lactose and α-la. The properties of the liquid film, which cannot be predicted by studying a single interface, are probably involved.

4.1.3. Pre-conditioning effects depend on sample composition

We have found that the pre-conditioning effects significantly depended on the protein composition. Pre-conditioned WPI samples had a significantly lower disproportionation rate than untreated samples, whereas the opposite was observed for β-lg (Fig. 9). In addition, two processing conditions resulted in particular behaviours as regards the interfacial properties, film dynamics and foam properties. As a matter of fact, WPI pre-conditioned at pH 3.5 yielded the highest interfacial storage modulus, the highest interfacial tension, the slowest film relaxation, the lowest yield stress and the lowest disproportionation rates of all the WPI samples.

Slight protein structural changes in solution and in the dry-state prior to dry heating may explain the pH pre-conditioning effects. For instance, conformational modifications occur in acidic conditions: a molten globule conformation for α-la and a dimerisation by intermolecular β-sheet for β-lg [22,55]. In addition, it has been shown an increase of lysozyme glycation when the pH prior to freeze-drying decrease (pH 6.2, 7.2, or 8.2) [56]. Some authors have suggested that lactosylation of β-lg may be limited by reducing the pH prior to drying [57].

Thus, protein physico-chemical changes due to pH adjustment could partly account for the variations in sample properties.

4.1.4. Impact of dry-heating on samples properties

We think that dry-heating generates aggregates and slight structural changes, which act simultaneously on the foam properties, through the bulk properties as well as the interface properties. Aggregates, upon competition with non-aggregated proteins, do not adsorb at interfaces [49].

We have shown that, whatever the sample composition, dry-heating decreased the interfacial elastic modulus. As discussed above, the interfacial dilatational elastic modulus E' mainly

depends on the intra-protein structural rigidity and the strength of inter-protein links formed during conformational rearrangements, which oppose interface compression and/or expansion. The higher the intra-protein structural rigidity, the higher the interfacial dilatational elasticity E'. Thus, all the treatments that promote protein unfolding lead to a decrease in E' [19]. Some authors have also demonstrated that dry-heating of egg-white powder induces a decrease in interfacial dilatational visco-elasticity [23].

We showed higher yield stress for WPI after dry-heating. That was not observed for β-lg. WPI dry-heated samples are likely to have larger aggregates than β-lg, even after the same heat treatment, due to the Maillard reaction [22]. Thus, larger aggregates for WPI may increase the strength of the protein network across the liquid film.

As regards the disproportionation rates, it has been shown that aggregates located at the interface, under specific pH condition and size, may decrease the rate of disproportionation but it was not observed in our study [49,58].

Overall, dry-heating had not a marked effect on interfacial properties and foam rheology, as compared with the effects of preconditioning. In addition, dry-heating could also modify the bulk properties through the possible formation of protein aggregates.

4.2. Multiscale correlations: Interfacial properties, film dynamics and bulk foam rheology

4.2.1. Film relaxation time and the interfacial dilatational elasticity and viscosity are correlated

It is worth noting that we report here the first measurements of the relaxation following a T1 event with proteins in the absence of added co-surfactant. Some authors have studied proteins solutions, but in the presence of polymers in order to prevent film rupture [33]. They observed longer relaxation times of $t_{90} \approx 3.7$ s, probably because of interactions between polysaccharides and proteins at the interface [59,60]. Our film relaxation measurements for different proteins in the absence of co-surfactant were made possible by using a high bulk protein concentration, more than ten times higher than in previous studies [33].

As shown in Fig. C in Supplementary data, relaxation times are independent of the bulk viscosity, as reported by Durand and Stone [33], meaning that the interfacial viscoelasticity is the main factor determining the relaxation kinetics. In particular, it has been demonstrated, for LMW surfactants, that the relaxation time is proportional to the ratio between the interfacial viscosity E'' and the interfacial tension [61].

As well, it should be noted that some authors have shown that an increase in liquid fraction inside the film may slow down the kinetics [10]. As an indirect method to monitor the film liquid fraction, we used image analysis to ensure that film thicknesses were not significantly different (see supplementary data, Table C). This led us to exclude NaCas, which was the only protein sample giving significantly thicker films.

A correlation test between the interfacial properties and relaxation time after a T1 are shown in Table 2 for β-lg and WPI samples.

Dilatational moduli E' and E'' and interfacial tension σ are both involved in foam properties. For this reason, we used the dimensionless interfacial elasticity E'/σ and interfacial viscosity E''/σ to characterise the interfacial properties.

It finally turns out that the highest and most significant correlations were obtained between the relaxation time after a T1 and both the dimensionless interfacial elasticity and interfacial viscosity at short aging times (Table 2). In other words, the higher the dimensionless interfacial elasticity and/or interfacial viscosity at short times, the slower the relaxation after a T1 event. In addition, it should be noted that these correlations were valid for the WPI as well as the purified β-lg.

Thus, the interfacial properties can be inferred indirectly through film relaxation by the five-film device.

4.2.2. Links between foam rheology, interfacial properties and film dynamics are sensitive to sample composition

In this part, we study the correlations between foam properties on the one hand and interfacial properties and film dynamics on the other hand.

As shown previously (Section 4.1), we observed an effect of the sample composition (β-lg or WPI) on interfacial properties, film dynamics and foam properties. It was thus necessary to separate β-lg samples from WPI samples in order to study the correlations between measurements at different scales.

In the case of β-lg samples (Table 3), several significant correlations exist between interfacial properties (direct measurements or indirect information through film relaxation) and the foam rheological properties. The dimensionless interfacial elasticity at short times as well as t_{90} are correlated with the foam storage and loss modulus, the disproportionation rate and the yield stress (Table 3). In other words, the higher the dimensionless interfacial elasticity, the longer the film relaxation after a T1 event, and the higher the disproportionation rate, the foam storage and loss moduli and the yield stress. Some of the correlations that we found for the β-lg samples are in agreement with results reported in the literature. Some studies on dairy proteins have reported that higher values of the interfacial dilatational elasticity (E') lead to an increased yield stress and foam modulus [46,48,62]. It has also been demonstrated with dry-heated egg-white that the higher the interfacial visco-elasticity (E' and E''), the higher the foam storage and loss moduli [23].

Table 2
Spearman's correlation coefficient r_s between t_{90} (the time for the film to reach 90% of its final length) and interfacial properties for β-lg and WPI samples.

	$(E'/\sigma)_{250\ s}$	$(E'/\sigma)_{1600\ s}$	$(E''/\sigma)_{250\ s}$	$(E''/\sigma)_{1600\ s}$
t_{90} (s)	0.90 ***	0.60 ***	0.74 ***	NS

| r_s | close to 1 means a stronger correlation. Significance depends on the p-value: *p < 0.05, **p < 0.01, ***p < 0.001. For a p-value > 0.05 correlation is considered as not significant (NS).

Table 3
Spearman correlation coefficient r_s between interfacial properties, foam rheology, disproportionation coefficient and T1 kinetics for all the β-lg samples.

	$(E'/\sigma)_{250\ s}$	$(E'/\sigma)_{1600\ s}$	$(E''/\sigma)_{250\ s}$	$(E''/\sigma)_{1600\ s}$	t_{90}
Disproportionation α	0.63 *	NS	NS	NS	0.70 *
Foam storage modulus G'_0	0.91 ***	0.85 ***	NS	NS	0.87 ***
Foam loss modulus G''_0	0.85 ***	0.76 **	NS	NS	0.82 ***
Yield strain	NS	NS	NS	NS	NS
Yield stress	0.76 **	0.73 **	NS	NS	0.61 *

| r_s | close to 1 means a stronger correlation. Significance depends on the p-value: *p < 0.05, **p < 0.01, ***p < 0.001. For a p-value > 0.05 correlation is considered as not significant (NS).

As regards the disproportionation rate, the correlations found for the β-lg samples are not fully consistent with the literature data. The rate of disproportionation decreases with an increase in the interface elasticity [46,58]. Martin et al. [15] have also reported that stability against disproportionation is correlated with higher dilatational elastic modulus E'. A higher ratio E'/σ should prevent bubble disproportionation [63]. However, for β-lg, our results show that increasing the dilatational elastic modulus E' increased the disproportionation rates.

As regards WPI, fewer significant correlations were obtained (see Supplementary data, Table D). As mentioned above (Section 4.1), due to its complex composition, complex dry-heating effects may be expected. As a consequence, other contributions than interfacial rheology, such as lamellar thickness, or intralamellar structure, may impact the foam properties.

As presented in Section 3.1 the interfacial properties of protein solutions are strongly time-dependent, whereas LMW surfactants quickly reach an equilibrium state at the interface [14]. Most of the significant correlations in Table 2 and 3 were found when considering the interfacial visco-elasticity well before a steady-state, plateau value. However, many studies on proteins report interfacial properties after 20–30 min [15,62,64]. Thus, the out-of-equilibrium and short time scale value of interfacial visco-elasticity and interfacial tension could be more relevant than "equilibrium" values to predict foam properties.

As mentioned in Section 3.3, in the general case, whatever the surfactant nature, the foam elastic modulus at low strain is supposed to be only a function of the liquid fraction [36,39,40], which would imply a constant value of the G'/(σ/R) for a given liquid fraction. We checked and discussed this relationship (supplementary data, Table B).

5. Conclusions

In the study of the general determinants of foam rheology and stability, proteins allow to explore a wider experimental domain than low-molecular-weight surfactants, especially as regards interfacial rheology. In the present work, the sensitivity of proteins to powder processing gave rise to a wide range of interfacial behaviours, allowing us to study correlations between interfacial properties, film dynamics and bulk foam rheology.

Interestingly, we found that the pre-conditioning of the samples prior to dry-heating accounts for the main source of differences, though it is not expected to induce major changes in the structural and physico-chemical properties of proteins. Thus, we think that slight structural protein modifications during pre-conditioning greatly impact the foam and interfacial properties of whey proteins in comparison with protein aggregates possibly produced during dry-heating. The pre-conditioning step may also result in subtle changes in the WPI composition, which can also be involved in changes in the interfacial and foam properties.

The novelty of our work is to transpose an approach from foam physics to food protein foams, in order to obtain a more detailed insight into the behaviour of protein foams. We showed that protein interfacial properties can be measured indirectly through film relaxation by the five-film device. In particular, it confirms that film relaxation has a central role in foam rheology and foam stability [7,10,51,61]. Thus, protein film relaxation after a T1 event can be considered as an intermediate scale between single interfaces and tridimensional foams, helpfully connecting interfacial properties to macroscopic foam properties. In addition, the use of foam rheology to infer the disproportionation rate may be an alternative to the bubble size characterisation during the foam aging [49].

We showed that β-lg foam mechanical properties, namely the foam storage and loss moduli and the yield stress, increase with the interfacial storage modulus, consistently with literature [46,48,62]. However, studies on purified β-lg, as a model protein, cannot fully explain the interfacial and foam properties of the WPI mixture. The presence of other proteins, lactose and minerals in WPI is likely to affect the protein behaviour at the interface and inside the liquid film, making the relationships between different length scales more complex.

Acknowledgements

We are grateful to the Regional council Bretagne (grant N° 13008651) and Regional council Pays de la Loire (grant N°2014-07081) for their financial support as well as INRA for its scientific coordination (J. Leonil) through the interregional project PROFIL, managed by the BBA industrial association. We thank Université Bretagne-Loire (UBL) for financing this research programme at Aberystwyth. We also warmly thank Marielle Harel-Oger, Fabienne Lambrouin, Benoît Robert an Jean-Luc Thomas for the successful and challenging project to purify β-lactoglobulin from milk. SJC is grateful for financial support from EPSRC (EP/N002326/1). We are grateful to J. Ashworth for making the T1 device.

Appendix A. Supplementary material

Supplementary data to this article can be found online at https://doi.org/10.1016/j.jcis.2019.02.006.

References

[1] P. Stevenson, Foam Engineering: Fundamentals and Applications, John Wiley & Sons, 2012.
[2] I. Cantat, S. Cohen-Addad, F. Elias, F. Graner, R. Höhler, O. Pitois, F. Rouyer, A. Saint-Jalmes, Foams: Structure and Dynamics, OUP, Oxford, 2013.
[3] S. Hutzler, D. Weaire, Foam coarsening under forced drainage, Philos. Mag. Lett. 80 (2000) 419–425, https://doi.org/10.1080/095008300403567.
[4] S.A. Koehler, S. Hilgenfeldt, H.A. Stone, A generalized view of foam drainage: experiment and theory, Langmuir 16 (2000) 6327–6341, https://doi.org/10.1021/la9913147.
[5] R. Höhler, S. Cohen-Addad, Rheology of liquid foam, J. Phys. Condens. Matter. 17 (2005) R1041, https://doi.org/10.1088/0953-8984/17/41/R01.
[6] A.D. Gopal, D.J. Durian, Shear-induced "Melting" of an aqueous foam, J. Colloid Interface Sci. 213 (1999) 169–178, https://doi.org/10.1006/jcis.1999.6123.
[7] B. Dollet, C. Raufaste, Rheology of aqueous foams, Comptes Rendus Phys. 15 (2014), https://doi.org/10.1016/j.crhy.2014.09.008.
[8] A.-L. Biance, A. Delbos, O. Pitois, How topological rearrangements and liquid fraction control liquid foam stability, Phys. Rev. Lett. 106 (2011), https://doi.org/10.1103/PhysRevLett. 106.068301.
[9] E. Rio, A.-L. Biance, Thermodynamic and mechanical timescales involved in foam film rupture and liquid foam coalescence, ChemPhysChem 15 (2014) 3692–3707, https://doi.org/10.1002/cphc.201402195.
[10] Z. Briceño-Ahumada, W. Drenckhan, D. Langevin, Coalescence in draining foams made of very small bubbles, Phys. Rev. Lett. 116 (2016). BIA.
[11] S. Hilgenfeldt, S.A. Koehler, H.A. Stone, Dynamics of coarsening foams: accelerated and self-limiting drainage, Phys. Rev. Lett. 86 (2001) 4704–4707, https://doi.org/10.1103/PhysRevLett. 86.4704.
[12] D. Langevin, Rheology of adsorbed surfactant monolayers at fluid surfaces, Annu. Rev. Fluid Mech. 46 (2014) 47–65, https://doi.org/10.1146/annurev-fluid-010313-141403.
[13] J. Wang, A.V. Nguyen, S. Farrokhpay, A critical review of the growth, drainage and collapse of foams, Adv. Colloid Interface Sci. 228 (2016) 55–70, https://doi.org/10.1016/j.cis.2015.11.009.
[14] M.A. Bos, T. van Vliet, Interfacial rheological properties of adsorbed protein layers and surfactants: a review, Adv. Colloid Interface Sci. 91 (2001) 437–471, https://doi.org/10.1016/S0001-8686(00)00077-4.
[15] A.H. Martin, K. Grolle, M.A. Bos, M.A.C. Stuart, T. van Vliet, Network forming properties of various proteins adsorbed at the air/water interface in relation to foam stability, J. Colloid Interface Sci. 254 (2002) 175–183, https://doi.org/10.1006/jcis.2002.8592.
[16] M. Lexis, N. Willenbacher, Relating foam and interfacial rheological properties of beta-lactoglobulin solutions, Soft Matter. 10 (2014) 9626–9636, https://doi.org/10.1039/c4sm01972e.
[17] Q. Wang, L. He, T.P. Labuza, B. Ismail, Structural characterisation of partially glycosylated whey protein as influenced by pH and heat using surface-enhanced Raman spectroscopy, Food Chem. 139 (2013) 313–319, https://doi.org/10.1016/j.foodchem.2012.12.050.
[18] S. Pezennec, F. Gauthier, C. Alonso, F. Graner, T. Croguennec, G. Brulé, A. Renault, The protein net electric charge determines the surface rheological

properties of ovalbumin adsorbed at the air–water interface, Food Hydrocoll. 14 (2000) 463–472, https://doi.org/10.1016/S0268-005X(00)00026-6.
[19] L.G. Cascão Pereira, O. Théodoly, H.W. Blanch, C.J. Radke, Dilatational rheology of BSA conformers at the air/water interface, Langmuir 19 (2003) 2349–2356, https://doi.org/10.1021/la020720e.
[20] S. Damodaran, Protein stabilization of emulsions and foams, J. Food Sci. 70 (2005) R54–R66, https://doi.org/10.1111/j.1365-2621.2005.tb07150.x.
[21] W. Zhang, P.R. Waghmare, L. Chen, Z. Xu, S.K. Mitra, Interfacial rheological and wetting properties of deamidated barley proteins, Food Hydrocoll. 43 (2015) 400–409, https://doi.org/10.1016/j.foodhyd.2014.06.012.
[22] F. Guyomarc'h, M.-H. Famelart, G. Henry, M. Gulzar, J. Leonil, P. Hamon, S. Bouhallab, T. Croguennec, Current ways to modify the structure of whey proteins for specific functionalities-a review, Dairy Sci. Technol. 95 (2015) 795–814, https://doi.org/10.1007/s13594-014-0190-5.
[23] E. Talansier, C. Loisel, D. Dellavalle, A. Desrumaux, V. Lechevalier, J. Legrand, Optimization of dry heat treatment of egg white in relation to foam and interfacial properties, LWT - Food Sci. Technol. 42 (2009) 496–503, https://doi.org/10.1016/j.lwt.2008.09.013.
[24] Y. Desfougères, A. Saint-Jalmes, A. Salonen, V. Vié, S. Beaufils, S. Pezennec, B. Desbat, V. Lechevalier, F. Nau, Strong improvement of interfacial properties can result from slight structural modifications of proteins: the case of native and dry-heated lysozyme, Langmuir 27 (2011) 14947–14957, https://doi.org/10.1021/la203485y.
[25] A. Audebert, S. Beaufils, V. Lechevalier, C. Le Floch-Fouéré, A. Saint-Jalmes, S. Pezennec, How foam stability against drainage is affected by conditions of prior whey protein powder storage and dry-heating: a multidimensional experimental approach, J. Food Eng. 242 (2019) 153–162, https://doi.org/10.1016/j.jfoodeng.2018.08.029.
[26] C. Bramaud, P. Aimar, G. Daufin, Thermal isoelectric precipitation of alpha-lactalbumin from a whey protein concentrate: Influence of protein-calcium complexation, Biotechnol. Bioeng. 47 (1995) 121–130, https://doi.org/10.1002/bit.260470202.
[27] G. Gésan-Guiziou, G. Daufin, M. Timmer, D. Allersma, C.V.D. Horst, Process steps for the preparation of purified fractions of α-lactalbumin and β-lactoglobulin from whey protein concentrates, J. Dairy Res. 66 (1999) 225–236.
[28] J. Toro-Sierra, A. Tolkach, U. Kulozik, Fractionation of α-lactalbumin and β-lactoglobulin from whey protein isolate using selective thermal aggregation, an optimized membrane separation procedure and resolubilization techniques at pilot plant scale, Food Bioprocess Technol. 6 (2013) 1032–1043, https://doi.org/10.1007/s11947-011-0732-2.
[29] C. Bhattacharjee, K.P. Das, Thermal unfolding and refolding of beta-lactoglobulin. An intrinsic andextrinsic fluorescence study, Eur. J. Biochem. 267 (2000) 3957–3964.
[30] M. Chevallier, A. Riaublanc, C. Lopez, P. Hamon, F. Rousseau, J. Thevenot, T. Croguennec, Increasing the heat stability of whey protein-rich emulsions by combining the functional role of WPM and caseins, Food Hydrocoll. 76 (2018) 164–172, https://doi.org/10.1016/j.foodhyd.2016.12.014.
[31] P. Schuck, R. Jeantet, A. Dolivet, Analytical Methods for Food and Dairy Powders, John Wiley & Sons, 2012. https://www.wiley.com/en-us/Analytical+Methods+for+Food+and+Dairy+Powders-p-9780470655986 (accessed February 8, 2018).
[32] W.S. Rasband, ImageJ, U. S. National Institutes of Health, Bethesda, Maryland, USA. https://imagej.nih.gov/ij/, 2016.
[33] M. Durand, H.A. Stone, Relaxation time of the topological $T1$ process in a two-dimensional foam, Phys. Rev. Lett. 97 (2006) 226101, https://doi.org/10.1103/PhysRevLett. 97.226101.
[34] J. Pierre, R.-M. Guillermic, F. Elias, W. Drenckhan, V. Leroy, Acoustic characterisation of liquid foams with an impedance tube, Eur. Phys. J. E Soft Matter. 36 (2013) 113, https://doi.org/10.1140/epje/i2013-13113-1.
[35] T. Gaillard, M. Roché, C. Honorez, M. Jumeau, A. Balan, C. Jedrzejczyk, W. Drenckhan, Controlled foam generation using cyclic diphasic flows through a constriction, Int. J. Multiph. Flow. 96 (2017) 173–187, https://doi.org/10.1016/j.ijmultiphaseflow.2017.02.009.
[36] A. Saint-Jalmes, D.J. Durian, Vanishing elasticity for wet foams: equivalence with emulsions and role of polydispersity, J. Rheol. 43 (1999) 1411–1422, https://doi.org/10.1122/1.551052.
[37] R Core Team, R: A language and environment for statistical computing, (2017). https://www.r-project.org/ (accessed May 16, 2018).
[38] V. Ulaganathan, I. Retzlaff, J.Y. Won, G. Gochev, D.Z. Gunes, C. Gehin-Delval, M. Leser, B.A. Noskov, R. Miller, β-Lactoglobulin adsorption layers at the water/air surface: 2. Dilational rheology: Effect of pH and ionic strength, Colloids Surf. Physicochem. Eng. Asp. 521 (2017) 167–176, https://doi.org/10.1016/j.colsurfa.2016.08.064.
[39] H.M. Princen, Rheology of foams and highly concentrated emulsions: I. Elastic properties and yield stress of a cylindrical model system, J. Colloid Interface Sci. 91 (1983) 160–175, https://doi.org/10.1016/0021-9797(83)90323-5.
[40] S. Marze, R.M. Guillermic, A. Saint-Jalmes, Oscillatory rheology of aqueous foams: surfactant, liquid fraction, experimental protocol and aging effects, Soft Matter. 5 (2009) 1937–1946, https://doi.org/10.1039/b817543h.
[41] A. Saint-Jalmes, Physical chemistry in foam drainage and coarsening, Soft Matter. 2 (2006) 836, https://doi.org/10.1039/b606780h.
[42] J. Pierre, B. Giraudet, P. Chasle, B. Dollet, A. Saint-Jalmes, Sound propagation in liquid foams: unraveling the balance between physical and chemical parameters, Phys. Rev. E. 91 (2015) 042311, https://doi.org/10.1103/PhysRevE.91.042311.
[43] N. Isert, G. Maret, C.M. Aegerter, Coarsening dynamics of three-dimensional levitated foams: From wet to dry, Eur. Phys. J. E. 36 (2013) 116, https://doi.org/10.1140/epje/i2013-13116-x.
[44] E.-A. Norwood, M. Chevallier, C. Le Floch-Fouéré, P. Schuck, R. Jeantet, T. Croguennec, Heat-induced aggregation properties of whey proteins as affected by storage conditions of whey protein isolate powders, Food Bioprocess. Technol. 9 (2016) 993–1001, https://doi.org/10.1007/s11947-016-1686-1.
[45] T. Coura Oliveira, S. Lopes Lima, J. Bressan, Influences of different thermal processings in milk, bovine meat and frog protein structure, Nutr. Hosp. 28 (2013) 896–902, https://doi.org/10.3305/nh.2013.28.3.5976.
[46] J.P. Davis, E.A. Foegeding, F.K. Hansen, Electrostatic effects on the yield stress of whey protein isolate foams, Colloids Surf. B-Biointerfaces 34 (2004) 13–23, https://doi.org/10.1016/j.colsurfb.2003.10.014.
[47] E. Dickinson, Y. Matsumura, Time-dependent polymerization of β-lactoglobulin through disulphide bonds at the oil-water interface in emulsions, Int. J. Biol. Macromol. 13 (1991) 26–30, https://doi.org/10.1016/0141-8130(91)90006-G.
[48] M. Lexis, N. Willenbacher, Yield stress and elasticity of aqueous foams from protein and surfactant solutions – The role of continuous phase viscosity and interfacial properties, Colloids Surf. Physicochem. Eng. Asp. 459 (2014) 177–185, https://doi.org/10.1016/j.colsurfa.2014.06.030.
[49] C. Schmitt, C. Bovay, M. Rouvet, S. Shojaei-Rami, E. Kolodziejczyk, Whey protein soluble aggregates from heating with NaCl: physicochemical, interfacial, and foaming properties, Langmuir 23 (2007) 4155–4166, https://doi.org/10.1021/la0632575.
[50] E. Dickinson, R. Ettelaie, B.S. Murray, Z. Du, Kinetics of disproportionation of air bubbles beneath a planar air-water interface stabilized by food proteins, J. Colloid Interface Sci. 252 (2002) 202–213, https://doi.org/10.1006/jcis.2002.8405.
[51] E. Rio, W. Drenckhan, A. Salonen, D. Langevin, Unusually stable liquid foams, Adv. Colloid Interface Sci. 205 (2014) 74–86, https://doi.org/10.1016/j.cis.2013.10.023.
[52] C. Schmitt, C. Bovay, M. Rouvet, Bulk self-aggregation drives foam stabilization properties of whey protein microgels, Food Hydrocoll. 42 (2014) 139–148, https://doi.org/10.1016/j.foodhyd.2014.03.010.
[53] B. Hiller, P.C. Lorenzen, Functional properties of milk proteins as affected by Maillard reaction induced oligomerisation, Food Res. Int. 43 (2010) 1155–1166, https://doi.org/10.1016/j.foodres.2010.02.006.
[54] M. Gulzar, S. Bouhallab, T. Croguennec, Structural consequences of dry heating on Beta-Lactoglobulin under controlled pH, Procedia Food Sci. 1 (2011) 391–398, https://doi.org/10.1016/j.profoo.2011.09.060.
[55] J.C. Ioannou, A.M. Donald, R.H. Tromp, Characterising the secondary structure changes occurring in high density systems of BLG dissolved in aqueous pH 3 buffer, Food Hydrocoll. 46 (2015) 216–225, https://doi.org/10.1016/j.foodhyd.2014.12.027.
[56] J.F. Povey, N. Perez-Moral, T.R. Noel, R. Parker, M.J. Howard, C.M. Smales, Investigating variables and mechanisms that influence protein integrity in low water content amorphous carbohydrate matrices, Biotechnol. Prog. 25 (2009) 1217–1227, https://doi.org/10.1002/btpr.207.
[57] M.K. Thomsen, K. Olsen, J. Otte, K. Sjøstrøm, B.B. Werner, L.H. Skibsted, Effect of water activity, temperature and pH on solid state lactosylation of β-lactoglobulin, Int. Dairy J. 23 (2012) 1–8, https://doi.org/10.1016/j.idairyj.2011.10.008.
[58] J. Dombrowski, F. Johler, M. Warncke, U. Kulozik, Correlation between bulk characteristics of aggregated beta-lactoglobulin and its surface and foaming properties, Food Hydrocoll. 61 (2016) 318–328, https://doi.org/10.1016/j.foodhyd.2016.05.027.
[59] D.K. Sarker, P.J. Wilde, Restoration of protein foam stability through electrostatic propylene glycol alginate-mediated protein–protein interactions, Colloids Surf. B Biointerfaces 15 (1999) 203–213, https://doi.org/10.1016/S0927-7757(99)00017-5.
[60] R. Baeza, C. Carrera Sanchez, A.M.R. Pilosof, J.M. Rodríguez Patino, Interactions of polysaccharides with β-lactoglobulin adsorbed films at the air–water interface, Food Hydrocoll. 19 (2005) 239–248, https://doi.org/10.1016/j.foodhyd.2004.06.002.
[61] A.-L. Biance, S. Cohen-Addad, R. Höhler, Topological transition dynamics in a strained bubble cluster, Soft Matter. 5 (2009) 4672, https://doi.org/10.1039/b910150k.
[62] K. Engelhardt, M. Lexis, G. Gochev, C. Konnerth, R. Miller, N. Willenbacher, W. Peukert, B. Braunschweig, pH effects on the molecular structure of β-lactoglobulin modified air-water interfaces and its impact on foam rheology, Langmuir 29 (2013) 11646–11655, https://doi.org/10.1021/la402729g.
[63] X. Yang, E.A. Foegeding, Effects of sucrose on egg white protein and whey protein isolate foams: factors determining properties of wet and dry foams (cakes), Food Hydrocoll. 24 (2010) 227–238, https://doi.org/10.1016/j.foodhyd.2009.09.011.
[64] J. Dombrowski, M. Gschwendtner, U. Kulozik, Evaluation of structural characteristics determining surface and foaming properties of β-lactoglobulin aggregates, Colloids Surf. Physicochem. Eng. Asp. 516 (2017) 286–295, https://doi.org/10.1016/j.colsurfa.2016.12.045.